Oxygen adsorption on the Ru(10$\bar{1}$0) surface: Anomalous coverage dependence

S. Schwegmann, A. P. Seitsonen, V. De Renzi, H. Dietrich, H. Bludau, M. Gierer, H. Over,* K. Jacobi, M. Scheffler, and G. Ertl

Fritz-Haber-Institut der Max-Planck-Gesellschaft, Faradayweg 4-6, D-14195 Berlin, Germany

(Received 18 August 1997; revised manuscript received 27 January 1998)

Oxygen adsorption on to Ru(10$\bar{1}$0) results in the formation of two ordered overlayers, i.e., a $c(2\times4)$-2O and a $(2\times1)p2mg$-2O phase, which were analyzed by low-energy electron diffraction (LEED) and density functional theory (DFT) calculation. In addition, the vibrational properties of these overlayers were studied by high-resolution electron loss spectroscopy. In both phases, oxygen occupies the threefold coordinated hcp site along the densely packed rows on an otherwise unreconstructed surface. The O atoms are attached to two atoms in the first Ru layer Ru(1) and to one Ru atom in the second layer Ru(2), forming zigzag chains along the troughs. While in the low-coverage $c(2\times4)$-O phase, the bond lengths of O to Ru(1) and Ru(2) are 2.08 and 2.03 Å, respectively, corresponding bond lengths in the high-coverage (2×1)-$p2mg$-2O phase are 2.01 and 2.04 Å (LEED). Although the adsorption energy decreases by 220 meV with O coverage (DFT calculations), we observe experimentally a shortening of the Ru(1)-O bond length with O coverage. The υ(Ru-O) stretch mode is found at 67 meV [$c(2\times4)$-2O] and 64 meV [$(2\times1)p2mg$-2O]. [S0163-1829(98)00824-8]

I. INTRODUCTION

The actual adsorption geometry of atoms and molecules at metal surfaces, i.e., the adsorption site and the bond lengths of an adsorbate to its attached substrate atoms, is essentially the result of a delicate balance between reaching the optimum surface charge density by the adsorbate, minimizing the Pauli repulsion between occupied orbitals of the adsorbate and the metal surface, and optimizing the electrostatic interaction between the adspecies.[1] If the charge density at the surface is modified, for example, due to coadsorbed atoms or molecules, the adsorption geometry of the preadsorbed species on the surface can vary widely. Illustrative examples have only recently been reported in the literature in that adsorption sites have shown to change upon coadsorption.[2] Not only in coadsorption systems but also in single-adsorbate systems the local bond configuration might vary with the density of adparticles since both the effective charge density at the surface and the adsorbate-adsorbate interaction may alter. Notable variations in the adsorption geometry of such homogeneous systems have been reported for alkali metal adsorption: For instance, with increasing coverage the adsorption site shifts either from on top to hcp sites, as for the case of Cs on Ru(0001) [Ref. 3(a)] or the coordination of adsorption is preserved, but still the adsorption site changes from fcc to hcp, as encountered with the system K/Ru(0001).[3(b)] Similar effects have been identified with density functional theory (DFT) calculations for alkali metal adsorption on the (111) and (100) surfaces of Al.[4]

With oxygen adsorption a change in adsorption site with coverage has not been identified so far, although for the O/Co(10$\bar{1}$0) system such a change from the fcc to hcp site was proposed on the basis of recent scanning tunneling microscopy (STM) and low-energy electron diffraction (LEED) investigations;[5] threefold coordinated fcc and hcp sites are characterized by one and two substrate atoms in the topmost layer, respectively. On Co(10$\bar{1}$0) oxygen forms a low-coverage $c(2\times4)$-2O phase, which on heating transforms irreversibly into a (2×1)-1O phase, and a high-coverage (2×1)-$p2mg$2O phase.[6] While the chemisorption of oxygen into hcp sites in the $(2\times1)p2mg$-2O phase has been recently confirmed with LEED,[7] the fcc adsorption site of $c(2\times4)$-2O still remains speculative, as it is only concluded from the high intensity of the LEED superstructure spots, which was interpreted in terms of strong lateral distortions of the substrate atoms.[5] On the Ru(10$\bar{1}$0) surface, which is much easier to prepare and to clean than Co(10$\bar{1}$0), oxygen adsorption also leads to the formation of $c(2\times4)$-2O and $(2\times1)p2mg$-2O overlayers.[8] However, the low O coverage phase on Ru(10$\bar{1}$0) is the thermodynamically stable one, while on Co(10$\bar{1}$0) the $c(2\times4)$-2O phase serves as a precursor state for the stable (but heavily reconstructed[9]) (2×1)-1O surface. Neither the clean Ru(10$\bar{1}$0) nor the oxygen-covered surfaces have been subjected to a LEED analysis so far. The motivation for the project discussed in this paper was to learn about the interaction of oxygen with the underlying Ru(10$\bar{1}$0) surface and about the modification of the local bonding configuration upon increasing the O coverage. For this purpose, we applied LEED for the determination of the atomic geometries, high resolution electron energy loss spectroscopy (HREELS) for examining the vibrational properties, and density functional theory (DFT) calculations to explore the energetics at this surface.

II. EXPERIMENTAL AND CALCULATIONAL DETAILS

A. LEED

The LEED experiments were conducted in a second ultrahigh-vacuum chamber (with base pressure 1×10^{-10} mbar) equipped with a four-grid LEED optics, a cylindrical mirror analyzer for Auger electron spectroscopy (AES), and facilities for surface cleaning and characterization. The LEED intensity data were recorded at 110 K using

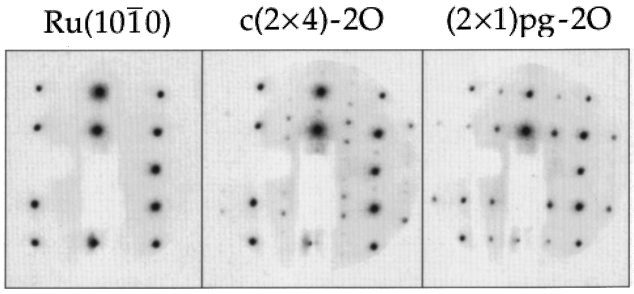

FIG. 1. LEED patterns of the (a) clean Ru(10$\bar{1}$0), (b) Ru(10$\bar{1}$0)-$c(2\times4)$-2O, and (c) Ru(10$\bar{1}$0)-$(2\times1)pg$-2O.

a video-LEED system.[10] The recorded LEED data were fed into a full-dynamical LEED program developed by Moritz[11] which is also equipped with a least-squares optimization scheme[12] in order to allow for the simultaneous and automated refinement of structural (as well as nonstructural) parameters. The degree of agreement between calculated and experimental data was judged by the reliability factors R_P (Ref. 13) and R_{de} (Ref. 14) which were also the quantities to be minimized in the optimization scheme. The scattering from Ru and O was treated by using up to nine phase shifts which were corrected for thermal vibrations by employing Debye temperatures of 420 K for Ru and 450 K for O. These temperatures were not refined during the analyses. The phase shifts have already been used in a previous LEED analysis of the (1×1)-O surface structures of Ru(0001).[15] The LEED analysis was carried out in two steps. First, an exhaustive grid search over a wide range in parameter space was conducted for both O phases with the unrelaxed substrate and the oxygen-ruthenium interlayer spacing being the only structural parameter. In the next step, starting from the optimum parameter values found by the grid searches, automated structure refinements were carried out. Apart from the first three layer spacings, lateral and vertical displacements of Ru atoms in the first and second layer (preserving the corresponding local symmetry of the adsorbate) were refined.

In both chambers (HREELS and LEED), the Ru(10$\bar{1}$0) sample was cleaned by argon ion bombardment at 1 keV followed by cycles of oxygen adsorption and thermal desorption in order to remove surface carbon. Final traces of oxygen were removed by flashing the surface to 1530 K, resulting in a sharp (1×1) LEED pattern (see Fig. 1) and no impurity losses in HREELS. The phases of $c(2\times4)$-2O and $(2\times1)pg$-2O were prepared by exposing the clean Ru(10$\bar{1}$0) at room temperature to 0.7 and 2.5 L oxygen, respectively (see Fig. 1). From AES measurements, the ratio of global oxygen coverages in the two ordered overlayers was 1:2. Together with the observation of a glide plane symmetry in the (2×1) phase, one can safely assume that both the $c(2\times4)$ and the (2×1) structure contain two O atoms in the unit cell. At room temperature, the (2×1) LEED pattern exhibits a glide symmetry plane along the [1$\bar{2}$10] direction, as inferred from the missing fractional-order spots $(n+1/2,0)$, $n=0,\pm1,\ldots$, at normal electron incidence; the proper nomenclature for this oxygen phase is therefore $(2\times1)pg$-2O.

By exposing the $(2\times1)pg$-2O structure to NO_2 at 500 K sample temperature, we tried to prepare an ordered O overlayer structure with coverage exceeding 1 ML. The same procedure has already been used successfully for the formation of the (1×1)-O structure on Ru(0001).[15] On Ru(10$\bar{1}$0), however, this procedure leads only to a streaky (1×2) phase in a wide O coverage range from 1.2 to 3–4 ML as estimated from AES and TDS measurements. Obviously, (1×1)-2O is not the most stable configuration at Ru(10$\bar{1}$0) under these experimental conditions, but it may exist as a metastable phase (see the DFT calculations below).

B. HREELS

The HREELS measurements were performed in an UHV apparatus with a base pressure of 2×10^{-11} mbar. The apparatus consists of two chambers. The upper chamber contains an argon ion gun, a quadrupole mass spectrometer, and a LEED optics. The lower chamber houses an HREELS spectrometer for recording the vibrational spectra which is capable of an energy resolution of $\Delta E=1$ meV in the reflected beam. The HREEL spectra were all taken at a 60° angle of incidence with respect to the surface normal and in specular geometry; the sample temperature was 293 K. The energy resolution was set to be 1.9 meV with typical counting rates of 3×10^5 counts per second in the elastic peak. In order to allow for direct comparison of HREELS and LEED results, the same sample and the same cleaning protocol were used.

C. DFT calculations

The density functional theory (DFT) calculations were performed using the generalized gradient approximation (GGA) of Perdew *et al.*[16] for the exchange-correlation functional. The action of the core electrons on the valence electrons was described by norm-conserving, fully relativistic pseudopotentials which were generated by the scheme of Troullier and Martins in the fully separable form;[17] the electronic wave functions were expanded in a plane-wave basis set. The used cutoff energy for the plane wave expansion of 50 Ry is sufficient to determine the adsorption energies with confidence, although the O-O interaction is not fully converged[18] even with a large pseudopotential core radius of $r_c{}^{l=0,1}=1.45$ bohr; $l=1$ was used as the local component. The core radii for the Ru pseudopotential are $r_c{}^{l=0,2}=2.48$ bohr and $r_c{}^{l=1}=2.78$ bohr; $l=0$ was used as the local component.[19] The **k**-point sampling of the surface Brillouin zone was accomplished with an equidistant 8×10 point Monkhorst-Pack grid[20] in the (1×1) unit cell, giving 20 **k** points in the irreducible part of the (1×1) Brillouin zone; special care was taken to ensure an equivalent sampling in all (surface) geometries studied. To stabilize the Brillouin zone integration the occupation numbers were broadened using a Fermi function with a width of 0.1 eV; the total energies were extrapolated to the case of no broadening. The surface was modeled using the supercell approach, using eight layers of Ru(10$\bar{1}$0) and placing the O atoms on one side of this slab. We account for the difference of the asymptotic electrostatic potential by employing a surface dipole correction.[21] The calculation scheme allows for relaxation of the electrons and atoms, where we relaxed the positions of the O atoms and the atoms in the top two Ru layers, keeping the lower five Ru layer spacings fixed at the bulk values. A similar procedure has shown to work reliably for the case of nitrogen adsorbed on Ru(0001).[22]

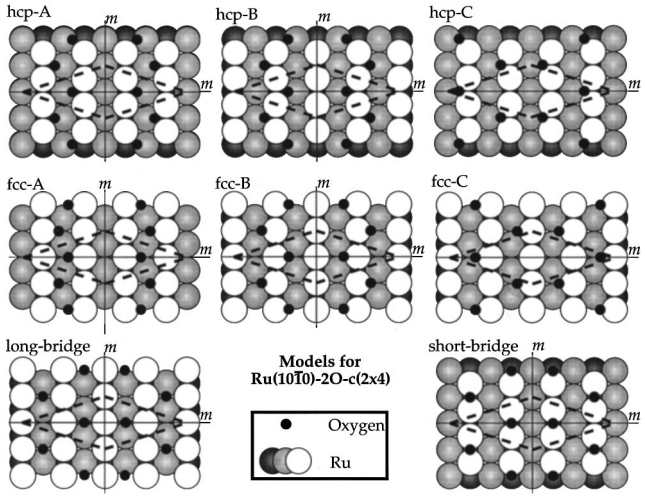

FIG. 2. Possible structure models for the Ru(10$\bar{1}$0)-$c(2\times4)$-2O, which were tested by LEED calculations.

III. RESULTS

A. LEED results

The analyses of the clean Ru(10$\bar{1}$0) surface and the oxygen-induced $c(2\times4)$-2O and $(2\times1)p2mg$-2O overlayers were based on experimental data sets containing cumulative energy ranges of 2165, 4525, and 3621 eV, respectively. In comparison with the oxygen Co(10$\bar{1}$0) system, one would not expect to find heavy reconstructions at the surface (recall that Ru is a much harder material than Co). Assuming only high-coordination adsorption sites for oxygen, we are left with eight substantially different models for the $c(2\times4)$-2O structure as compiled in Fig. 2. The presence of the glide symmetry plane in the $(2\times1)p2mg$-2O overlayer imposes constraints to the structure which further narrows down the number of possible models depicted in Fig. 3. We should note that the glide symmetry plane disappeared reversibly upon cooling below 230 K; this interesting issue will be the subject of a future paper.[23] For this reason we took the LEED IV data of the $(2\times1)p2mg$-2O phase at 250 K.

The clean Ru(10$\bar{1}$0) surface was analyzed first. Two different terminations of the (10$\bar{1}$0) surface are possible, exhibiting different corrugations of about 0.8 Å (short termination) and 1.6 Å (long termination), respectively. From a comparison with the surface geometries of Re(10$\bar{1}$0) (Ref. 24) and Co(10$\bar{1}$0),[25] we anticipated that only the short-termination with a small corrugation will be stable. The measurements of LEED IV curves at 110 K turned out to be complicated, due to small amounts of contaminants arising from the residual gas adsorption, as the LEED IV curves changed quite notably after a few minutes. Yet, using these IV curves for the LEED analysis, we ended with an optimum structure for which the topmost Ru layer spacing is almost bulklike. This finding conflicts with the results of about 10% contraction obtained for the topmost Re and Co layer distance on (10$\bar{1}$0). The best fit was achieved with the expected short termination giving an overall Pendry R factor of 0.25. From AES measurements, which indicated a clean surface, we concluded that very likely hydrogen, which is inevitably present in the residual gas, should be responsible for this effect. Therefore, we recorded a further set of LEED IV data at 430 K, a temperature at which hydrogen is not stabilized at the surface. With these new LEED data a much better fit to the experimental data was achieved, i.e., $R_P=0.18$, and in addition, the structural parameters were now consistent with corresponding results for Co and Re. The topmost Ru layer spacing turned out to be contracted by 10 ± 1.5 % followed by a small expansion of 2.5% of the second Ru layer spacing in good agreement with the DFT calculations (see Sec. III C).

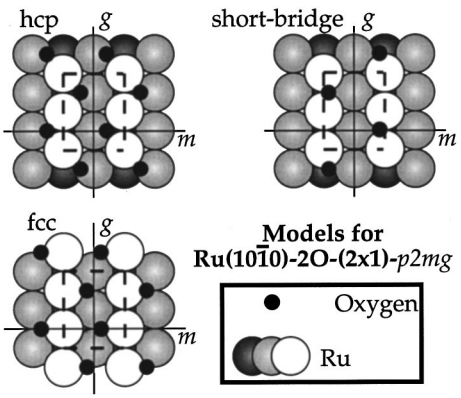

FIG. 3. Possible structure models for the Ru(10$\bar{1}$0)-$(2\times1)p2mg$-2O, which were tested by LEED calculations.

TABLE I. Optimum Pendry r factors obtained for different models of the Ru(10$\bar{1}$0)-2O-c(2×4). The total energy range is 4525 eV (2445 eV fractional-order, 2080 eV integer-order beams).

	R_p		
adsorption sites	total	integer	fractional
fcc A	0.65	0.30	0.94
fcc B	0.66	0.30	0.94
fcc C	0.66	0.29	0.96
hcp A	0.26	0.20	0.33
hcp B	0.57	0.30	0.83
hcp C	0.50	0.24	0.76
long bridge	0.74	0.39	1.02
short bridge	0.68	0.42	0.91

Next, we focus on the atomic geometry of the $c(2\times4)$-2O phase on Ru(10$\bar{1}$0). The various model structures considered in this LEED analysis are summarized in Fig. 2; all of these models provide at least one mirror plane across the densely packed Ru rows in [1 2 $\bar{1}$0] direction. Only high-symmetry adsorption sites were tested. The best r factors reached with these models are listed in Table I, from which it becomes clear that the model with oxygen sitting in so-called hcp sites is preferred. The optimum adsorption geometry is presented in Fig. 4, and the agreement between experimental and calculated LEED data can be judged from Fig. 5; the overall r factor is $R_P=0.26$. The chemisorption of oxygen induces only small lateral (up to 0.05 Å) and vertical (up to 0.03 Å) displacements of atoms in the top double layer. The oxygen atoms form zigzag chains along the troughs. Zigzag and zagzig chains are separated by an empty trough establishing the $c(2\times4)$ symmetry. The alternation

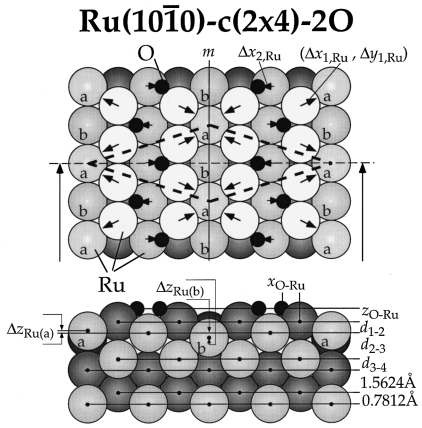

Parameter	LEED	DFT
x_{O-Ru} (Å)	1.19 ± 0.06	1.18
z_{O-Ru} (Å)	1.02 ± 0.03	1.05
$\Delta x_{2,Ru}$ (Å)	0.01 ± 0.03	(0.00)
$\Delta x_{1,Ru}$ (Å)	0.04 ± 0.06	(0.00)
$\Delta y_{1,Ru}$ (Å)	0.02 ± 0.06	(0.00)
$\Delta z_{Ru(a)}$ (Å)	0.03 ± 0.03	0.02
$\Delta z_{Ru(b)}$ (Å)	0.02 ± 0.03	0.00
d_{1-2} (Å)	0.75 ± 0.04	0.76
d_{2-3} (Å)	1.54 ± 0.02	1.59
d_{3-4} (Å)	(0.7812)	0.80

FIG. 4. The atomic coordinates for the best-fit model of $c(2\times4)$-2O as obtained by quantitative LEED and DFT-GGA calculations. Oxygen atoms reside in hcp-like adsorption sites forming zigzag chains along the troughs. Zigzag and zagzig chains are separated by empty troughs so that no oxygen atom has to share a Ru atom in the topmost layer with neighboring O atoms. The oxygen bond lengths to first-layer and second-layer Ru atoms are 2.08 and 2.03 Å, respectively. The relative O and Ru radii are scaled.

of zigzag and zagzig chains is necessary to impose $c(2\times4)$ symmetry, otherwise a primitive (2×2) structure would have been formed. At temperatures above 550 K the $c(2\times4)$-O structure disorders as indicated by LEED while the $(2\times1)p2mg$ persists up to desorption. The formation of oxygen zigzag chains along the troughs maximizes the separation between oxygen atoms within the troughs, although the overall O-O separation is not maximized; from this point

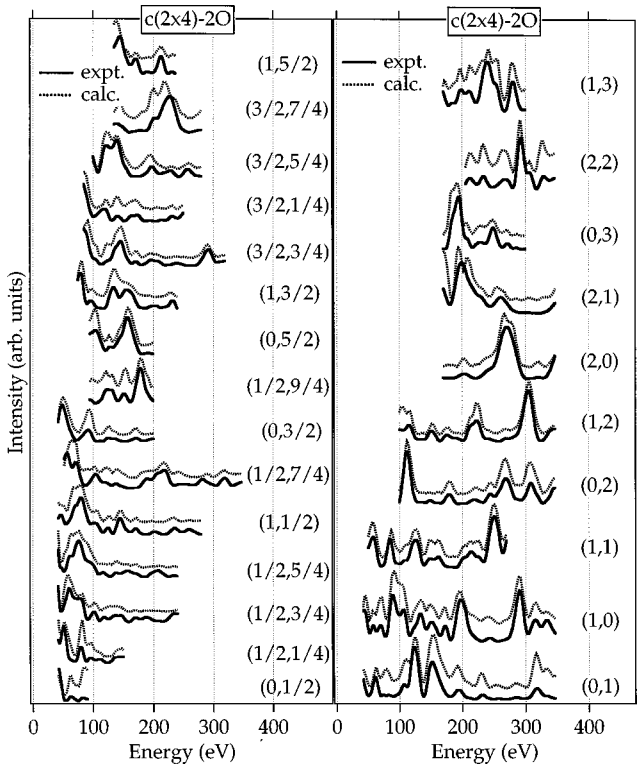

FIG. 5. Comparison of experimental and theoretical LEED IV data for the best-fit model of the $c(2\times4)$-2O phase on Ru(10$\bar{1}$0) (cf. Fig. 4). The overall R_P factor is 0.26.

TABLE II. Optimum Pendry r factors obtained for different models of the Ru(10$\bar{1}$0)-2O-$(2\times1)p2mg$. The total energy range is 3621 eV (1464 eV fractional-order, 2157 eV integer-order beams).

	R_p		
adsorption sites	total	integer	fractional
fcc	0.71	0.55	0.95
hcp	0.25	0.23	0.29
short bridge	0.69	0.56	0.87

of view model hcp-c, see Fig. 2, would be more favorable. The bond lengths of oxygen to first-layer Ru atoms and second-layer Ru atoms is (2.08± 0.06) Å and (2.03 ± 0.06) Å, respectively. The contraction (10%) of the topmost Ru layer spacing of the clean Ru(10$\bar{1}$0) is partly lifted upon adsorption of oxygen, resulting in a contraction of about 4%.

The structural characteristics of the $c(2\times4)$-2O phase are to be compared with the adsorption geometry of the second ordered oxygen overlayer, i.e., the $(2\times1)pg$-2O. For modeling this oxygen overlayer, only three different models (Fig. 3) have to be considered. The corresponding optimum r factors are compiled in Table II. Clearly, also here the hcp site is most favored. The actual adsorption geometry determined by LEED is presented in Fig. 6, and a comparison between experimental and calculated LEED data is depicted in Fig. 7 (the overall r factor is $R_P=0.25$). The presence of the glide symmetry plane determines the lateral arrangement of the O atoms to consist again of O zigzag chains along the [1$\bar{2}$10] direction. The main differences to the $c(2\times4)$-2O configuration are the absence of empty troughs and the exclusive occurrence of zigzag chains (and no zagzig chains). Therefore, the $c(2\times4)$-2O phase transforms into the $(2\times1)p2mg$-2O phase by filling up the empty troughs by O zigzag chains and shifting every zagzig chain of the

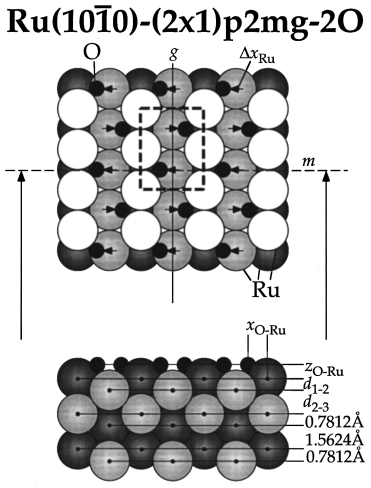

Parameter	LEED	DFT
x_{O-Ru} (Å)	1.13 ± 0.05	1.19
z_{O-Ru} (Å)	0.96 ± 0.02	1.06
Δx_{Ru} (Å)	0.03 ± 0.04	(0.00)
d_{1-2} (Å)	0.81 ± 0.01	0.81
d_{2-3} (Å)	1.53 ± 0.02	1.58

FIG. 6. The atomic coordinates for the best-fit model of $(2\times1)p2mg$-2O, as determined by LEED and DFT. Oxygen atoms reside in hcp-like adsorption sites forming zigzag chains along the troughs. The oxygen bond lengths to first-layer and second-layer Ru atoms are 2.01 and 2.04 Å, respectively. The relative O and Ru radii are scaled.

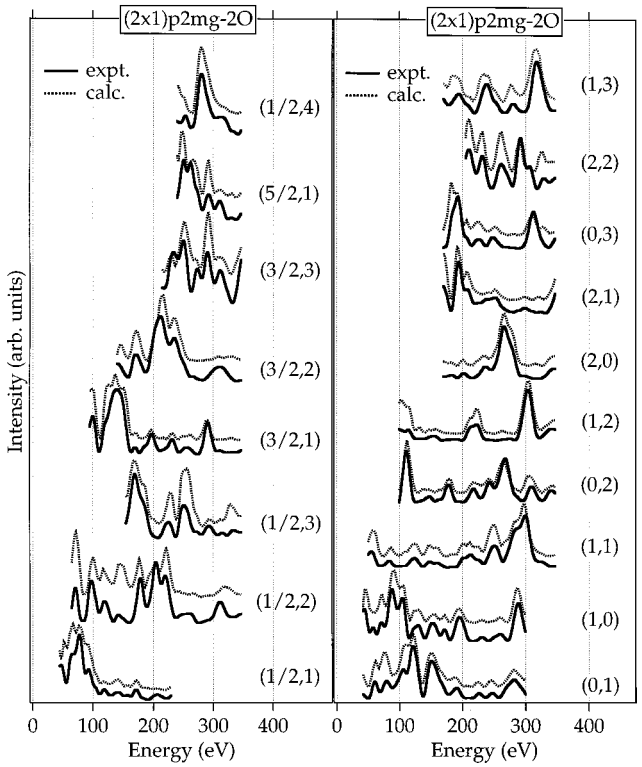

FIG. 7. Comparison of experimental and theoretical LEED IV data for the best-fit model of the $(2\times1)p2mg$-2O phase on Ru(10$\bar{1}$0) (cf. Fig. 6). The overall R_P factor is 0.25.

$c(2\times4)$-2O along the [1$\bar{2}$10] direction by one lattice unit. In contrast to the $c(2\times4)$-2O surface, the high-coverage $(2\times1)p2mg$-2O phase is thermally very stable and exists, up to desorption. Besides these general features of the oxygen arrangement, the bond lengths between oxygen and the first-layer and second-layer Ru atoms amount to 2.01 $\pm$0.06 Å and 2.04$\pm$0.06 Å, respectively. As with the $c(2\times4)$-2O, oxygen induces only little local reconstructions in the top Ru double layer. The topmost Ru layer spacing is now slightly expanded by 4%.

B. HREELS results

In order to study the vibrational properties of chemisorbed oxygen on Ru(10$\bar{1}$0), HREEL spectra were recorded. A characteristic set of spectra is shown in Fig. 8. The main energy loss is found at 64 to 67 meV and is assigned to the Ru-O stretch mode perpendicular to the surface ν(Ru-O). With progressing oxygen exposure, this mode shifts from 67 down to 64 meV. At an oxygen dose of 10 L, it broadens and obviously contains several contributions. The observed energy compares well with the value of 64 meV found for the low-coverage mode ($\theta_O=0.25$) of atomic oxygen on Ru(0001).

Between 70 and 100 meV, a broad band of losses with low intensities is present, which exhibits peaks at 86 and 95 meV for the 2×1 structure. The weak loss at 95 meV occurs already for the smallest dose of 0.1 L. In analogy to the work of Mitchell and Weinberg,[26] we tentatively assign these losses to subsurface oxygen. Besides the main ν(Ru-O) stretch mode and the features at higher energies, peaks at

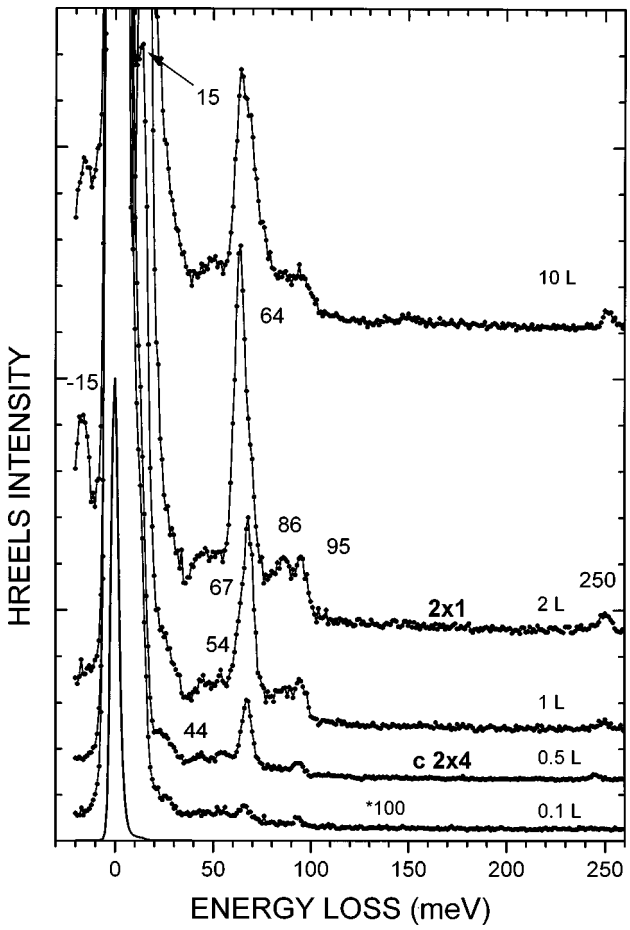

FIG. 8. HREEL spectra for a series of oxygen exposures on Ru(10$\bar{1}$0) at room temperature. The exposures and the monitored LEED patterns are indicated in the figure. All spectra are recorded in specular geometry with primary energy of 2.5 eV. The scaling factor in the loss region is 100.

13–15, 23, 44, and 54 meV are assigned to phonons of the oxygen-modified Ru(10$\bar{1}$0) surface.[26] The weak peak around 250 meV is assigned to the ν(C-O) stretch mode from background CO.

C. DFT calculations

The lattice parameters were calculated using a unit cell related to the (10$\bar{1}$0) surface. The results obtained, $a=2.78$ Å and $c/a=1.58$, are very close to our values for the Ru(0001) surface, thus confirming a good **k**-point sampling. The overestimation of a by about 2–3%, compared to the experiment, is frequently found in DFT-GGA calculations for later $4d$ transition metals.

As, to the best of our knowledge, this is the first DFT calculation for a clean transition metal (10$\bar{1}$0) surface, we shall elaborate on this issue here to some extent. The clean Ru surface was modeled using an eight-layer slab, and the two first substrate layers were relaxed. The hcp(10$\bar{1}$0) surface is a more open surface than the hexagonal, close-packed (0001) surface, and there are two possible terminations. As expected (due to higher coordination of surface atoms and smaller surface corrugation), the short termination is energetically favored by 41 meV/Å^2 over the long-terminated surface. The surface energy of the short termination is calcu-

TABLE III. Oxygen adsorption energy, work function change, and O-Ru distances in different overlayer structures. The adsorption energy is calculated with respect to a free oxygen molecule. Ru(1) denotes the outermost-layer Ru atoms and Ru(2) the second-layer atoms. In the structure (1×1)-2O (hcp-fcc) we give the average of the distances from the atom at the hcp/fcc site to the Ru atoms.

structure	coverage	E_{ad} (eV)	$\Delta\Phi$ (eV)	d[O-Ru(1)] (Å)	d[O-Ru(2)] (Å)
$c(2\times4)$-2O	**0.50**	**2.81**	**0.69**	**2.09**	**2.10**
(2×2)-2O	0.50	2.75	0.65	2.08	2.11
(2×1)-1O	0.50	2.75	0.69	2.07	2.14
(2×1)p2mg−2O	**1.00**	**2.59**	**1.61**	**2.11**	**2.11**
(1×1)-1O hcp	1.00	2.53	1.16	2.07	2.09
(1×1)-1O fcc	1.00	2.30	0.74	2.04	2.11
(1×1)-2O hcp	2.00	1.37	1.33	2.01	2.10
(1×1)-2O hcp-fcc	**2.00**	**1.47**	**1.91**	**1.98**	**2.08**

lated as 176 meV/Å^2 which is ≈15% larger than our DFT-GGA surface energy for the Ru(0001) surface (154 meV/Å^2). Note that DFT-GGA yields lower surface energies than DFT-LDA and it appears that LDA is in better agreement with experiments.[27] The relaxations of the first and second layer turned out to be $d_{12}/d_0=-13.7\%$ and $d_{23}/d_0=-0.7\%$, thus, a slightly larger inward relaxation is obtained than from the LEED intensity data ($d_{12}/d_0\approx-10\%$). Similar deviations have also been observed with Ru(0001).[28,29] The inclusion of the effects of zero-point vibration and thermal expansion[30] in the calculations further reduces the difference between theory and experiment: at $T=300$ K, the first-layer contraction amounts to $d_{12}/d_0=-12.3\%$ which agrees with the experiments within the error bars. The calculated work function of 4.88 eV is somewhat too low compared to the experiment, 5.10 eV,[31] again as also observed in DFT-GGA calculations of other metals.[27]

To study the adsorption of oxygen, we have considered several coverages and overlayer arrangements. They are compiled in Table III, together with the adsorption energies per O atom and work function changes with respect to the clean surface. In addition to the experimentally observed surface structures, we also studied some hypothetical structures in order to gain additional information about the adsorbate-adsorbate interaction. From Table III, we see that the adsorption energy decreases upon oxygen adsorption, while the work function increases. Even the (1×1)-2O phase is found to be stable. This is no surprise, as the oxygen atoms are bound on threefold hollow sites as on the Ru(0001) surface, and the density of adsorbates is close to the one in the Ru(0001)-(1×1)-O structure, which was also found to be stable.[15,29] It is interesting that the energetically lowest (1×1)-2O structure on Ru(10$\bar{1}$0) contains both atoms adsorbed on the hcp and fcc sites, whereas in the (1×1)-1O structure the hcp site is clearly preferred. The occupation of fcc and hcp sites in the (1×1)-2O phase maximizes the separation between the O atoms within the troughs and therefore minimizes the electrostatic O-O repulsion. Yet, the LEED experiments did not give evidence for the presence of a (1×1)-2O structure. Therefore, one might conjecture that the excess oxygen atoms partly penetrate into the subsurface region at a sample temperature of 550 K leading to the diffuse and streaky (1×2) LEED pattern.

Comparing the nearest-neighbor distance and the adsorption energy of the $(2\times1)pg$-2O with the (1×1)-1O, we find the energy gain by forming zigzag chains to be 60 meV per oxygen atom, which is consistent with a reduction of the O-O repulsion. The binding energy per adsorbate increases by 220 meV per atom, when the coverage is reduced from 1 to $\frac{1}{2}$. However, the $c(2\times4)$-2O structure, where the zigzag and zagzig chains alternate, is preferred (60 meV) over the (2×2)-2O exhibiting zigzag chains only.

Next, we are focusing on the O-Ru distances as a function of coverage. The O-Ru distances in the $c(2\times4)$ phase are d[O-Ru(1)]=2.09 Å and d[O-Ru(2)]=2.10 Å, while in the $(2\times1)pg$ structure these distances are d[O-Ru(1)]=2.11 Å and d[O-Ru(2)]=2.11 Å. These bond lengths are slightly longer than in the experiment $c(2\times4)$-2O:d[O-Ru(1)]=2.08 Å/d[O-Ru(2)]=2.03 Å; **(2×1)***p*2*mg*:d[O-Ru(1)]=2.03 Å and d[O-Ru(2)] =2.03 Å), which might be due to the DFT-GGA scheme. In disagreement with the experiments, the bond lengths do not vary noticeably, when going from the $c(2\times4)$-2O to the $(2\times1)p2mg$-2O structure. Specific values for the atomic coordinates as determined by DFT-GGA calculations are indicated in Figs. 4 and 6. However, going to even higher O coverages, DFT-GGA calculations also indicate a decreasing O-Ru distance. DFT-GGA calculations of the system O/Ru(0001) (Refs. 29 and 32) show that the O-Ru bond strength decreases monotonically with increasing O coverage.

Using the same pseudopotentials as for O/Ru(10$\bar{1}$0), the binding energies of oxygen on Ru(0001) turned out to be 3.08 and 2.29 eV and the Ru-O bond lengths are 2.07 and 2.04 Å in the (2×2)-O and the (1×1)-O phase, respectively. The slightly larger Ru-O binding energy in the Ru(0001)-(2×2)-O phase compared to Ru(10$\bar{1}$0)-$c(2\times4)$-O might be due to the larger O-O separation.

In addition to the above DFT-GGA calculations, we analyzed the binding of oxygen on Ru(10$\bar{1}$0) by using a simple tight-binding model,[33] which we recently applied to N/Ru(0001).[22] The qualitative result is the same (see Fig. 9), i.e., the bond splits the mixed adsorbate-substrate orbitals—mainly O_{2p} and Ru_{4d}—into a bonding level below and an antibonding level above the Fermi level, emptying some Ru_{4d} orbitals just below the Fermi energy. The position of

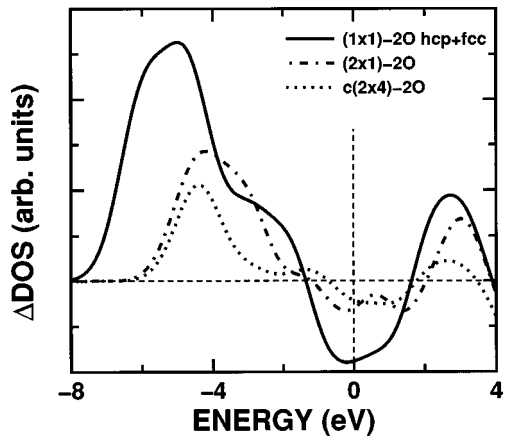

FIG. 9. The difference in density of states $n(\mathrm{Ru+O})-n(\mathrm{Ru})$, where $n(\mathrm{Ru+O})$ is the density of states of the adsorbate system Ru(10$\bar{1}$0)-$(2\times1)p2mg$-O (dotted-dashed line), Ru(10$\bar{1}$0)-(1×1)-(fcc+hcp)2O (solid line), Ru(10$\bar{1}$0)-$c(2\times4)$-2O (dotted line), and $n(\mathrm{Ru})$ that of the clean Ru surface. The one-electron eigenvalues are broadened by 0.6 eV.

the bonding orbital shifts from $E_F-5.5$ eV [$c(2\times4)$-2O] to $E_F-6.5$ eV [(1×1)-2O] with increasing coverage. The antibonding peak is at $E_F+2.5$ eV in the $c(2\times4)$-2O structure and shifts slightly to higher energies when increasing the coverage. Both shifts are in agreement with the smaller O-Ru distance upon increasing the O coverage (taken from Table III), if one neglects the effective repulsion between the oxygen atoms.

IV. DISCUSSION

The interaction of oxygen with the substrate and neighboring oxygen atoms can be classified in three categories according to the sequence of their importance, namely the direct coordination shell of oxygen, the formation of O-zigzag chains, coverage dependent changes of O-Ru bonding, and last the correlation between the zigzag chains. Starting point of the discussion will be the structural results, as provided by the LEED method, which is followed by a critical comparison between LEED and corresponding results of DFT calculations and HREELS measurements. Special emphasis will be placed on the relation between structural and energetic properties of the O-Ru(10$\bar{1}$0) system, applying simple tight binding and effective medium theory (EMT) arguments.

(1) Oxygen binds to the Ru substrate via two atoms in the topmost Ru layer and one in the second layer as identified by LEED and DFT. Such an adsorption site may also be the adsorption site in the limit of zero coverage. Obviously, oxygen prefers to form bonds to the low-coordinated Ru atoms of the topmost layer. This finding may be explained in the following way. The local charge density of the low-coordinated Ru atoms Ru(1) at the surface is larger than of high-coordinated Ru atoms Ru(2), since less charge density is supplied to the internal bonds between the Ru atoms (tight binding argument). Using now simple effective medium theory (EMT) arguments, which have been put forward by Nørskov and coworkers,[1a,34] the bonding between oxygen and Ru depends critically on the local charge density offered by the substrate: The more local charge density is available, the longer the O-Ru bond length and the smaller the Pauli repulsion. Also this aspect of the Ru-O bonding is retrieved by the present LEED analysis of the Ru(10$\bar{1}$0)-$c(2\times4)$-2O overlayer. The bond length of O to Ru(1) with 2.08 Å is markedly longer than between O and Ru(2) (2.03 Å). On the Ru(0001) surface all Ru atoms are high coordinated, i.e., the local charge density is low, and as expected the O-Ru bond length of Ru(0001)-(2×2)-O [LEED: 2.03 Å (Ref. 35)] is quite short and virtually identical to the O-Ru(2) value on Ru(10$\bar{1}$0). This simple view is further supported by the O-induced reconstructions on Ru(10$\bar{1}$0) which are much less pronounced than on Ru(0001).[35] Obviously, on Ru(10$\bar{1}$0) oxygen atoms can readily reach the optimum charge density without shifting the Ru atoms too much. Yet, this interpretation within the framework of local charge density is not conclusive, as the present DFT calculations (which are certainly superior over EMT calculations in terms of accuracy) cannot reconcile this behavior for reasons which are unknown: DFT calculations show almost no variation in the O-Ru bond length with the coordination of the Ru atoms (see Table III). However, DFT calculations show that the hcp adsorption site of oxygen is favored by more than 0.2 eV over the fcc site [see Table III, (1×1)1O-fcc and (1×1)1O-hcp].

(2) The next important contribution to the Ru-O bond is related to the formation of zigzag chains along the troughs. These zigzag arrangements were also observed for hydrogen on fcc(110) surfaces, such as Ni(110) (Ref. 36) and oxygen on Rh(110) (Ref. 37), and it therefore seems a quite common structural motif in surface crystallography. LEED and HREELS measurements indicate that even at lower O coverages these chains are preferentially formed on Ru(10$\bar{1}$0). This observation is also supported by the DFT calculations which indicated that the formation of zigzag chains is by 60 meV per oxygen atom more favorable than single O atoms. This means that the interaction between the oxygen atoms along the zigzag chains is attractive.

(3) In spite of the attractive O-O interaction, oxygen does not like to share attached Ru atoms with other oxygen atoms. This attribute is manifested by the presence of empty trough between the zigzag and zagzig chains observed for the $c(2\times4)$-2O system. If, however, the O coverage is increased, the empty troughs are filled up with the consequence that oxygen atoms have to share common Ru atoms in the topmost layer. Accordingly, the local charge density offered by Ru(1) atoms for each O atom is smaller and, again using the simple arguments from EMT of bonding, this tells us that now the oxygen atoms have to come closer to the substrate to experience a similar local charge density as in the $c(2\times4)$-2O phase. In fact, this aspect has been identified in the LEED analysis, the bond lengths of O to Ru(1) change from 2.08 to 2.01 Å, when going from the $c(2\times4)$-2O to the (2×1)-$p2mg$-2O phase. The bonding between the oxygen atom and the coordinated Ru(2) atom is not affected by the presence of more oxygen on the surface, as evidenced by the unchanged bond length of 2.03 Å and consistent with the unchanged coordination shell of Ru(2).

All these findings cannot be easily reconciled with simple arguments adopted from coordination chemistry, since there the bond length is directly related to the bond strength: The weaker the bonding, the longer the respective bond length.

The present DFT calculations show, however, that the binding energy of oxygen is reduced by about 220 meV, when the oxygen coverage is increased and two oxygen atoms have to share one Ru atom in the topmost layer. According to coordination chemistry, the O-Ru(1) and O-Ru(2) bond lengths should increase which, however, conflicts with the present LEED results. One should recall that the total Ru-O binding energy is the results of both the direct O-Ru interaction and the O-O repulsion. Hence, a situation is conceivable where the direct O-Ru interaction increases with coverage (consistent with a shorter bond length) but the total adsorption energy still decreases, because of the stronger electrostatic O-O repulsion. However, from the mere observation of zigzag chains even at low O coverages (indicative of O-O attraction) one may infer that the O-O repulsion is only of minor importance (see also the discussion of the work function change below).

Unfortunately, the present DFT calculations are not able to elaborate on this interesting issue, as the optimum Ru-O bond length turned out not to change with O coverage when the $c(2\times4)$-2O phase transforms into the $(2\times1)p2mg$-2O phase. It could be that such an effect is beyond the capability of state-of-the-art DFT-GGA calculations. As possible sources for this discrepancy we mention just the exchange correlation term, the frozen-core approximation, the linearization of the core-valence exchange correlation, and the transferability of the pseudopotentials in our DFT calculations. Although the variation of the Ru(1)-O bond length with O coverage (as determined by LEED) is similar to the quoted error bars for the Ru(1)-O bond lengths, simple probability arguments, i.e., taking the product probability, tell that the found variation is statistically significant: the probability to find the Ru(1)-O bond length to increase is only 20%.

An alternative explanation for the observed shortening of the Ru(1)-O bond length with O coverage could be that with increasing O coverage the ionicity of O decreases. Consequently, the Pauling radius of oxygen would shrink compatible with a smaller Ru-O bond length. This explanation fails, however, to explain the observed change of the work function $\Delta\Phi$. Using ultraviolet photoelectron spectroscopy[38] it was shown that $\Delta\Phi$ increases from 0.49 eV [$c(2\times4)$-2O] to 1.12 eV [$(2\times1)pg$-2O] with respect to the clean surface. This superlinear increase of the oxygen induced dipole moment conflicts with a reduced degree of ionicity in combination with a smaller Ru-O bond length, i.e., smaller dipole length. It is worth mentioning that this superlinear change of the work function induced by oxygen is nicely reproduced by the present DFT calculations (see Table III). An increase of the oxygen induced dipole moment with coverage indicates that the electrostatic O-O repulsion is not very important since direct O-O repulsion always tries to reduce the dipole moment via depolarization (see the discussion in Ref. 21).

A shortening of the Ru-O bond length with coverage has recently been identified for oxygen on Ru(0001) by LEED and DFT.[15,35] While the O-Ru bond length in both the (2×2) and the (2×1) phase was 2.03 Å,[35] this bond length shortens to 2.00 Å for the (1×1)-O structure, although the binding energy decreases by more than 0.8 eV, as evidenced by DFT calculations. Obviously, local coordination chemistry considerations, which would predict that the stronger the bond, the shorter the bond length, are inadequate to account for the bonding of oxygen atoms at the Ru surfaces.

On Ru(10$\bar{1}$0) the Ru-O stretch mode changes its energy only slightly from 67 to 64 meV when going from the $c(2\times4)$-2O to $(2\times1)p2mg$-2O phase, i.e., the steepness of the potential normal to the surface does not change very much. This small change might be attributed to the smaller total bond strength of oxygen to the Ru surface in the $(2\times1)p2mg$-2O than in the $c(2\times4)$-2O, as indicated by the present DFT calculation. The frequency is very close to that one for the low-coverage oxygen phase on Ru(0001) (64 meV at $\theta_O=0.25$). Only when the lateral nearest-neighbor O-O distance on Ru(0001) changes from 5.72 Å ($\theta_O=0.25$) to 2.71 Å, the ν(Ru-O) mode energy changes to 71 meV ($\theta_O=0.50$) and 81 meV ($\theta_O=1.00$).[39] For Ru(10$\bar{1}$0) the nearest-neighbor distances remain quite large in both phases: 3.30 Å in the $c(2\times4)$-2O and 3.38 Å in the $(2\times1)p2mg$-2O. Therefore, the ν(Ru-O) mode energy is nearly constant.

(3) Last, we discuss the interaction which determines the correlation between the zigzag and zagzig chains in the $c(2\times4)$-2O phase. As demonstrated by LEED, this interaction can easily be overcome by increasing the surface temperature above 550 K, where also the correlation between the O atoms within the zigzag chains is destroyed. DFT calculations indicate that this energy contribution is with 60 meV per oxygen atom [see Table III: $c(2\times4)$-2O and (2×2)-2O] indeed comparable to the O-O attraction within the troughs. Disordering of the $(2\times1)p2mg$ phase, on the other hand, would bring O atoms in adjacent troughs too close to each other which is energetically disfavored by about 0.8 eV [see Table III: (1×1)-1O-hcp and (1×1)-2O-hcp] and is therefore not observed experimentally. As demonstrated by LEED, the $(2\times1)p2mg$ phase is stable up to oxygen desorption.

V. SUMMARY

The $c(2\times4)$-2O and the $(2\times1)p2mg$-2O phases on Ru(10$\bar{1}$0) were characterized by using quantitative LEED and DFT-GGA calculations, which were supplemented by HREELS measurements. We have shown that in both phases oxygen atoms occupy the threefold coordinated hcp site along the densely packed rows on an otherwise unreconstructed surface, i.e., the O atoms are attached to two atoms in the first Ru layer Ru(1) and to one Ru atom in the second layer Ru(2). With LEED we found that in the low-coverage $c(2\times4)$-O phase the bond lengths of O to Ru(1) and Ru(2) are 2.08 and 2.03 Å, respectively, while corresponding bond lengths in the high-coverage $(2\times1)p2mg$-2O phase are 2.01 and 2.04 Å. The shortening of the Ru(1)-O bond length with O coverage may be a consequence of the competition for electron charge density, although this aspect could not be reconciled by the present DFT calculations. The occurrence of empty troughs in the $c(2\times4)$-2O phase indicates that oxygen atoms do not like to share Ru atoms with other O atoms. DFT calculations show that the energy per O atom in both phases differs by 220 meV. An energy gain of 60 meV drives the O atoms to build zigzag chains along the troughs instead of a dispersed O phase. A similar energy contribution is gained when forming alternating zigzag and zagzig chains

instead of zigzag chains only. HREEL spectra reveal a loss at 67 meV [$c(2\times4)$-2O] and 64 meV [$(2\times1)p2mg$-2O], which is assigned to the ν(Ru-O) stretch mode. The small variation in frequency with O coverage [compared to a much bigger shift for the oxygen phases on Ru(0001)] reflects the similar lateral arrangements of oxygen in both phases on Ru(10 1 0), i.e., the formation of zigzag chains.

ACKNOWLEDGMENTS

We thank R. Stumpf for valuable discussions and K. Christmann for bringing the experimental work function changes of O-Ru(10 1 0) (Ref. 38) to our attention. V.D. acknowledges partial financial support by the A. Della Riccia Foundation.

*Author to whom correspondence should be sent. Fax: ++49-30-84135106. Electronic address: over@fhi-berlin.mpg.de

[1] See e.g., (a) J. K. Nørskov, Rep. Prog. Phys. **53**, 1253 (1990); (b) M. J. Stott and E. Zaremba, Phys. Rev. B **22**, 1564 (1980); (c) M. W. Finnis and J. E. Sinclair, Philos. Mag. A **50**, 45 (1984); (d) F. Ducastelle and F. Cyrot-Lackmann, J. Phys. Chem. Solids **32**, 285 (1971); (e) F. Ercolessi, E. Tosatti, and M. Parrinello, Phys. Rev. Lett. **57**, 719 (1986); (f) I. J. Robertson, M. C. Payne, and V. Heine, *ibid.* **70**, 1944 (1993).

[2] B. Narloch, G. Held, and D. Menzel, Surf. Sci. **317**, 131 (1994); H. Over, H. Bludau, R. Kose, and G. Ertl, Phys. Rev. B **51**, 4661 (1995).

[3] H. Over, H. Bludau, M. Skottke-Klein, G. Ertl, W. Moritz, and C. T. Campbell, Phys. Rev. B **45**, 8638 (1992); M. Gierer, H. Bludau, T. Hertel, H. Over, W. Moritz, and G. Ertl, Surf. Sci. **279**, L170 (1992).

[4] C. Stampfl and M. Scheffler, Surf. Rev. Lett. **2**, 317 (1995).

[5] R. Koch, B. Burg, K.-H. Rieder, and E. Schwarz, Mod. Phys. Lett. B **8**, 571 (1994).

[6] E. Schwarz, K. H. Schwarz, C. Gonser-Buntrock, M. Neuber, and K. Christmann, Vacuum **41**, 180 (1990).

[7] M. Gierer, H. Over, P. Rech, E. Schwarz, and K. Christmann, Surf. Sci. **370**, L201 (1997).

[8] T. W. Orent and R. S. Hansen, Surf. Sci. **67**, 325 (1977).

[9] R. Koch, E. Schwarz, K. Schmidt, B. Burg, K. Christmann, and K.-H. Rieder, Phys. Rev. Lett. **71**, 1047 (1993).

[10] K. Müller, E. Lang, L. Hammer, W. Grimm, P. Heilmann, and K. Heinz, in *Determination of Surface Structure by LEED*, edited by P. M. Marcus and F. Jona (Plenum, New York, 1984).

[11] W. Moritz, J. Phys. C **17**, 353 (1983).

[12] G. Kleinle, W. Moritz, and G. Ertl, Surf. Sci. **238**, 119 (1990); H. Over, U. Ketterl, W. Moritz, and G. Ertl, Phys. Rev. B **46**, 15 438 (1992); M. Gierer, H. Over, and W. Moritz (unpublished).

[13] J. B. Pendry, J. Phys. C **13**, 937 (1980).

[14] G. Kleinle, W. Moritz, D. L. Adams, and G. Ertl, Surf. Sci. **219**, L637 (1989).

[15] C. Stampfl, S. Schwegmann, H. Over, M. Scheffler, and G. Ertl, Phys. Rev. Lett. **77**, 3371 (1996).

[16] J. P. Perdew, J. A. Chevary, S. H. Vosko, K. A. Jackson, M. R. Pederson, D. J. Singh, and C. Fiolhais, Phys. Rev. B **46**, 6671 (1992).

[17] N. Troullier and J. L. Martins, Phys. Rev. B **43**, 1991 (1993).

[18] The binding energy and bond length of O_2 in the gas phase are well converged while the vibrational frequency is not. The Ru-O bonds at the surface are also well converged and the O-O interaction on the surface is partially screened by the substrate and not important due to the large O-O separation.

[19] Note that in the DFT calculation of Ref. 31 the same pseudopotential for Ru, but a slightly different pseudo potential for oxygen was taken ($r_c^{l=0,1}=1.35$ bohr).

[20] H. J. Monkhorst and J. D. Pack, Phys. Rev. B **13**, 5188 (1976).

[21] J. Neugebauer and M. Scheffler, Phys. Rev. B **46**, 16 067 (1992).

[22] S. Schwegmann, A. P. Seitsonen, H. Dietrich, H. Bludau, H. Over, K. Jacobi, and G. Ertl, Chem. Phys. Lett. **264**, 680 (1997).

[23] S. Schwegmann, V. De Renzi, H. Bludau, H. Over, and G. Ertl (unpublished).

[24] H. L. Davis and D. M. Zehnder, J. Vac. Sci. Technol. **17**, 190 (1980).

[25] H. Over, G. Kleinle, W. Moritz, G. Ertl, K.-H. Ernst, H. Wohlgemuth, K. Christmann, and E. Schwarz, Surf. Sci. **254**, L469 (1991).

[26] W. J. Mitchell and W. H. Weinberg, J. Chem. Phys. **104**, 9127 (1996).

[27] M. Fuchs and M. Scheffler (unpublished).

[28] G. Michalk, W. Moritz, H. Pfnür, and D. Menzel, Surf. Sci. **129**, 92 (1983).

[29] C. Stampfl and M. Scheffler, Phys. Rev. B **54**, 2868 (1996).

[30] J.-H. Cho and M. Scheffler, Phys. Rev. Lett. **78**, 1299 (1997); S. Narasimhan and M. Scheffler (unpublished).

[31] K. Jacobi, in *Physics of Solid Surfaces*, edited by G. Chiarotti, Landolt Börnstein, Group-III Vol. 24, Pt. B (Springer, Berlin-Heidelberg, 1994), p. 277.

[32] A. P. Seitsonen (unpublished).

[33] R. Hoffmann, Rev. Mod. Phys. **60**, 601 (1988).

[34] K. W. Jacobsen, J. K. Nørskov, and M. J. Puska, Phys. Rev. B **35**, 7423 (1987); B. Hammer and J. K. Nørskov, in *Chemisorption and Reactivity on Supported Clusters and Thin Films: Towards an Understanding of Microscopic Processes in Catalysis*, Vol. 331 of *NATO Advanced Study Institute, Series E: Applied Sciences*, edited by R. Lambert and G. Pacchioni (Kluwer, Amsterdam, 1997), p. 285.

[35] H. Pfnür, G. Held, M. Lindroos, and D. Menzel, Surf. Sci. **220**, 43 (1990); M. Lindroos, H. Pfnür, G. Held, and D. Menzel, *ibid.* **222**, 451 (1989).

[36] V. Penka, K. Christmann, and G. Ertl, Surf. Sci. **136**, 307 (1984).

[37] M. Gierer, H. Over, G. Ertl, H. Wohlgemuth, E. Schwarz, and K. Christmann, Surf. Sci. Lett. **279**, L73 (1993).

[38] P. Rech, Ph.D. thesis, FU Berlin, 1996.

[39] P. He and K. Jacobi, Phys. Rev. B **55**, 4751 (1997).